Title
Competing magnetic orders in the superconducting state of heavy-fermion CeRhIn5.

Authors
Rosa, P
Kang, J
Luo, Yongkang
et al.

Peer reviewed

Competing magnetic orders in the superconducting state of heavy-fermion CeRhIn$_5$

P. F. S. Rosa[a], J. Kang[b], Yongkang Luo[a], N. Wakeham[a], E. D. Bauer[a], F. Ronning[a], Z. Fisk[c,1], R. M. Fernandes[b], and J. D. Thompson[a]

[a]Material Physics and Applications–Condensed Matter and Magnet Science, Los Alamos National Laboratory, Los Alamos, NM 87545; [b]School of Physics and Astronomy, University of Minnesota, Minneapolis, MN 55455; and [c]Department of Physics and Astronomy, University of California, Irvine, CA 92697-4574

Applied pressure drives the heavy-fermion antiferromagnet CeRhIn$_5$ toward a quantum critical point that becomes hidden by a dome of unconventional superconductivity. Magnetic fields suppress this superconducting dome, unveiling the quantum phase transition of local character. Here, we show that 5% magnetic substitution at the Ce site in CeRhIn$_5$, either by Nd or Gd, induces a zero-field magnetic instability inside the superconducting state. This magnetic state not only should have a different ordering vector than the high-field local-moment magnetic state, but it also competes with the latter, suggesting that a spin-density-wave phase is stabilized in zero field by Nd and Gd impurities, similarly to the case of Ce$_{0.95}$Nd$_{0.05}$CoIn$_5$. Supported by model calculations, we attribute this spin-density wave instability to a magnetic-impurity-driven condensation of the spin excitons that form inside the unconventional superconducting state.

magnetism | superconductivity | heavy fermions

Unconventional superconductivity (SC) frequently is found as an antiferromagnetic (AFM) transition is tuned by chemical substitution or pressure toward a zero-temperature phase transition, a magnetic quantum-critical point. This observation has a qualitative explanation: The proliferation of quantum fluctuations of magnetic origin at low temperatures can trigger the formation of a new ordered state. Unconventional SC is a natural candidate state because it can be induced by an attractive Cooper-pair interaction provided by the fluctuating magnetism (1, 2). Typical examples include copper oxides, which, without chemical substitution, are AFM Mott insulators (3), metallic iron-based antiferromagnets that superconduct under pressure or with chemical substitutions (4), and rare-earth and actinide-based heavy-fermion compounds with large effective electronic masses (5).

A characteristic manifestation of the unconventional nature of the superconducting state is the momentum dependence of the SC gap Δ that develops below the superconducting transition temperature (T_c). In contrast to conventional superconductors, Δ is not uniform but instead has different signs in different regions of the Fermi surface. Despite the distinct chemical and electronic properties of these materials, the interplay between magnetism and SC is common among them, calling for a deep understanding of this relationship. In this regard, heavy-fermion materials offer an ideal platform to explore the relationship between these two phases.

An additional common feature among these different classes of superconductors is the emergence of a collective magnetic excitation below T_c often attributed to the formation of a spin exciton (see a review in ref. 6). This collective mode, whose energy has been shown to scale with Δ across different materials (7), is a direct consequence of the sign-changing nature of Δ. An example is the heavy-fermion superconductor CeCoIn$_5$, known to be very close to an AFM quantum-critical point without tuning (5). Indeed, its SC gap is sign-changing (8–10), and a spin resonance mode is observed below T_c (11). The energy of this mode in CeCoIn$_5$ scales with its SC gap with the same proportionality found in copper oxide- and iron-based systems (7).

Recent inelastic neutron scattering experiments find that the resonance mode in CeCoIn$_5$ is incommensurate at the wavevector $\mathbf{Q} = (0.45, 0.45, 0.5)$ (12). Due to Ce's $4f$ crystal-field environment, this mode is a doublet and the corresponding fluctuations are polarized along the c axis. When a magnetic field H is applied in the tetragonal ab plane, this mode splits into two well-defined branches (13, 14). The field dependence of the Zeeman-split lower-energy mode extrapolates to zero energy at ~ 110 kilo-oersted (kOe), which is remarkably close to the field where long-range AFM order develops inside the low-T, high-H SC state (15–17). Spin-density wave (SDW) order in this so-called Q phase has a small c-axis ordered moment of 0.15 Bohr magneton (μ_B), which corresponds closely to the spectral weight of the low-energy resonance mode. Moreover, the SDW displays the same incommensurate wavevector $\mathbf{Q}$ as the spin resonance mode (16). These observations suggest that the Q phase is the result of a condensation of spin excitations (12, 14, 18).

In addition to the field-induced Q phase, AFM order is found in Ce$_{0.95}$Nd$_{0.05}$CoIn$_5$ below T_c, in this case at zero field (19). The wavevector and moment size of the Nd-induced magnetism are the same as those observed in the Q phase of CeCoIn$_5$ (20). Although the sign-changing Δ, with its nodes on the Fermi surface, plays a nontrivial role in enabling these orders, the obvious similarity between H- and Nd-induced magnetism strongly

Significance

Discovering new interdependences among magnetism, unconventional superconductivity and quantum criticality presents new insights into how electronic matter can organize itself into unexpected quantum states but also poses a fundamental challenge to current understanding. Here, we show that two qualitatively different types of magnetic order develop inside the pressure-induced superconducting state of Ce$_{0.95}$Nd$_{0.05}$RhIn$_5$. Field-induced magnetic order, derived from Cerium's $4f$ electrons, competes with zero-field, spin-density order that forms by condensation of magnetic excitations in a spin resonance. The zero-field magnetism is tuned to quantum-critical points by pressure and magnetic field. These discoveries portend possibilities for new quantum states arising from magnetic orders and quantum criticality in other unconventional superconductors that host a spin resonance.

suggests that they have a common origin, namely condensation of the collective spin excitations that give rise to the resonance mode.

No evidence for the Q phase has been found in other $CeMIn_5$ members ($M = $ Rh, Ir) or, for that matter, in any other superconductor. It is uncommon to find a magnetic transition below T_c when both superconducting and magnetic states arise from the same electrons. Besides the example of $CeCoIn_5$, field-induced magnetism has been observed in $La_{1.9}Sr_{0.1}CuO_4$ (21, 22). This AFM order, however, is distinct from a Q-like phase and is closely related to the field-induced magnetism in the SC state of pressurized $CeRhIn_5$ (23). At zero pressure, $CeRhIn_5$ displays AFM order at $T_N = 3.8$ K and $\mathbf{Q}_{AFM} = (0.5, 0.5, 0.297)$ (24). Pressurizing $CeRhIn_5$ tunes its magnetic transition toward a quantum-critical point and induces SC that coexists with AFM order for pressures up to $P_{c1} = 1.75$ GPa, where T_c equals T_N. Above P_{c1}, evidence for T_N is absent and only SC is observed (23, 25, 26). Application of a magnetic field, however, induces magnetism in the SC state between P_{c1} and the quantum-critical point at $P_{c2} \approx 2.3$ GPa (23, 27). Unlike magnetic order in the Q phase, which exists only inside the SC state, field-induced magnetism in $CeRhIn_5$ persists into the normal state above the Pauli-limited H_{c2} and is a smooth continuation of the zero-field $T_N(P)$ boundary (23, 27). This magnetism may obscure or pre-empt the formation of a Q-like phase, but strong similarities of $CeCoIn_5$ to $CeRhIn_5$ at $P > P_{c1}$ (23, 28) suggest the possibility that AFM order might develop in the high-pressure SC state of $Ce_{1-x}Nd_xRhIn_5$ in zero field.

In this paper, we show that Nd induces a zero-field phase transition in the high-pressure SC phase of $Ce_{0.95}Nd_{0.05}RhIn_5$ and present evidence that the phase transition is due to magnetic order. This result generalizes the observation of magnetic order below T_c in $Ce_{0.95}Nd_{0.05}CoIn_5$ because pressure suppresses the magnetic order at the same rate in both compounds. Our model calculations support our conclusion that the magnetism in Nd-doped $CeRhIn_5$ is due to the condensation of spin excitations promoted by magnetic impurity scattering, and is thus distinct from the local-moment magnetism in pure $CeRhIn_5$ promoted by the application of magnetic fields. In agreement with this proposal, we observe a competition between the field-induced magnetism, which displays the same behavior as in $CeRhIn_5$, and the Nd-induced magnetism in zero field. Hence, we expect a spin resonance with c-axis character below T_c in $CeRhIn_5$ at pressures greater than P_{c1}. More generally, our work reveals a route to induce zero-field magnetic order via chemical substitution of magnetic impurities in other unconventional superconductors that host spin resonance modes.

Results

For comparison with $Ce_{0.95}Nd_{0.05}CoIn_5$, we grew crystals of $Ce_{0.95}Nd_{0.05}RhIn_5$ by an In-flux technique (29) and studied its pressure and field dependence by electrical resistivity and AC calorimetry measurements (see *Materials and Methods* for details). Fig. 1A shows the low-temperature electrical resistivity, $\rho(T)$, on sample s1 at representative pressures, and Fig. 1A, *Inset* displays $\rho(T)$ in the whole T range. Although Nd substitution reduces $T_N(P = 0)$ from 3.8 K to 3.4 K and slightly increases the residual resistivity ρ_0 to 0.2 $\mu\Omega$·cm, the P dependence reported in Fig. 1A is essentially identical to that of $CeRhIn_5$ below $P_{c1}^* = 1.8$ GPa where T_c equals T_N. We also note that, at zero pressure, the $H - T$ phase diagram of $Ce_{0.95}Nd_{0.05}RhIn_5$ closely resembles the one found in $CeRhIn_5$. These results indicate that 5% Nd does not change drastically the local AFM character of T_N below P_{c1}^*. Once T_c exceeds T_N at P_{c1}^*, there is no evidence for magnetism in $\rho(T)$, and the possibility of Nd-induced magnetism is obscured by the zero-resistance state below T_c. To investigate whether there is AFM order in the SC state, heat capacity measurements are necessary.
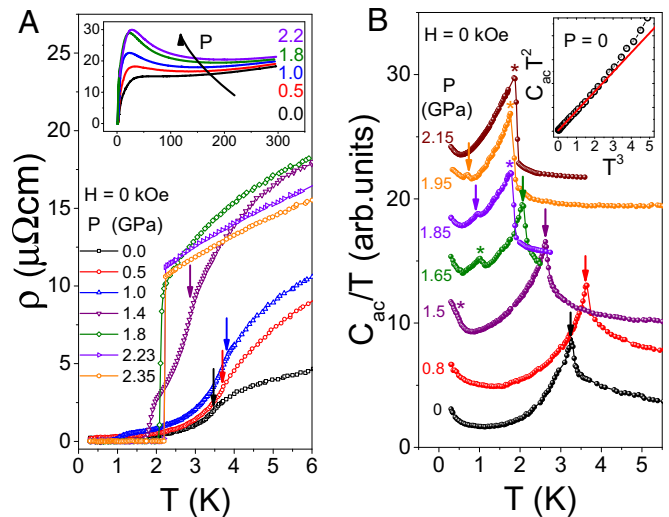

Fig. 1. (*A*) Low-T dependence of the in-plane electrical resistivity, $\rho(T)$, of $Ce_{0.95}Nd_{0.05}RhIn_5$ (s1) under pressure. Arrows mark T_N determined by peaks in the first derivative. (*Inset*) The $\rho(T)$ over the entire T-range. (*B*) C_{ac}/T vs T for $Ce_{0.95}Nd_{0.05}RhIn_5$ (s2) under pressure. A vertical offset of 2.5 units is added for clarity. Arrows (asterisks) denote T_N (T_c). (*Inset*) A linear fit in a $C_{ac}T^2$ vs T^3 plot.

Fig. 1B shows the T dependence of heat capacity divided by temperature (C_{ac}/T) for sample s2 at various pressures. At ambient pressure, C_{ac}/T peaks at T_N as in $CeRhIn_5$. As T is lowered further, however, C_{ac}/T turns up below ~ 1 K, which was not observed in $CeRhIn_5$. We note that an upturn in C/T also has been observed in a commercial quantum design physical property measurement system (PPMS) by means of quasiadiabatic thermal relaxation technique. This upturn is presumably associated with the nuclear moment of Nd ions, and it can be fit well by a sum of electronic ($\propto \gamma$) and nuclear ($\propto T^{-3}$) terms (30). Fig. 1B, *Inset* shows that $C_{ac}T^2$ is linear in T^3, consistent with the presence of a nuclear Schottky contribution. We note, however, that an upturn also is observed at 2.15 GPa, where magnetic order is absent, suggesting that the hyperfine field may not be solely responsible for splitting the nuclear levels. Although Nd nuclei have large zero-field quadrupole moments, Kondo-hole physics cannot be ruled out as a possible source of the upturn (31, 32).

For pressures below P_{c1}^*, T_N evolves with P as it does in transport data. Evidence for bulk SC (marked by asterisks in Fig. 1B), however, is observed at lower temperatures relative to the zero-resistance state in $\rho(T)$. A difference between zero-resistance and bulk SC transitions also appears in $CeRhIn_5$ and has been attributed to filamentary SC due to the presence of long-range AFM order (33). Unlike $CeRhIn_5$ at pressures greater than P_{c1}, however, there is evidence for a phase transition in the SC state of $Ce_{0.95}Nd_{0.05}RhIn_5$ without an applied field. At 1.85 GPa, an anomaly in C_{ac}/T is observed at 1 K (arrow in Fig. 1B), below the SC transition at $T_c = 1.77$ K. For reasons discussed below, this anomaly stems from a magnetic order, and it is fundamentally different from the AFM order displayed by the system for pressures smaller than P_{c1}. The shape and magnitude of the anomaly relative to that at T_c are very similar to those at T_N in $Ce_{0.95}Nd_{0.05}CoIn_5$ (see *Supporting Information*, Fig. S1), and the small entropy associated with it suggests that the magnetic order is most likely a small-moment density wave. As we will come to later, this evidence is most obvious in data shown in Fig. 3.

We summarize the zero-field results discussed above in the $T-P$ phase diagram shown in Fig. 2. Local-moment-like AFM order coexists with bulk SC in a narrow pressure range below
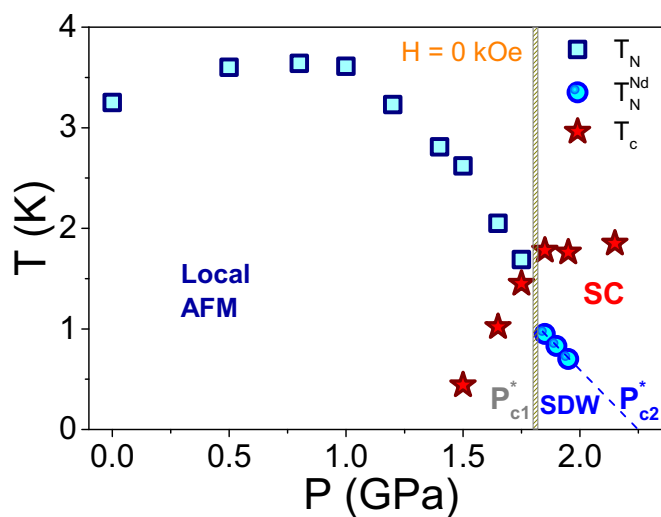
Fig. 2. Zero-field T–P phase diagram of $Ce_{0.95}Nd_{0.05}RhIn_5$ (s2) obtained from AC calorimetry measurements. Here, $P_{c1}^* \approx 1.8$ GPa and $P_{c2}^* \approx 2.3$ GPa.

P_{c1}^*. From just below to just above P_{c1}^*, $T_N(P)$ changes discontinuously, in contrast to field-induced magnetism in CeRhIn$_5$, which is a smooth continuation of $T_N(P)$ from below P_{c1} (23). This result supports the interpretation that H- and Nd-induced magnetic orders have different origins. Therefore, the Nd-induced transition is labeled T_N^{Nd} to distinguish it from T_N in pure CeRhIn$_5$. Above P_{c1}^*, T_N^{Nd} is suppressed at a rate of -2.4 K/GPa and extrapolates to zero temperature, i.e., a quantum-critical point, at $P_{c2}^* \sim 2.3$ GPa inside the superconducting phase. Whether the coincidence of P_{c2}^* and P_{c2} is accidental or not requires further investigation beyond the scope of our work. As shown in the *Supporting Information* (Fig. S1), the rate of suppression of this Nd-induced transition is the same rate found in $Ce_{0.95}Nd_{0.05}CoIn_5$ within experimental uncertainty, strongly indicating a common origin. Because entropy associated with the zero-field transition is rather small, as found in $Ce_{1-x}Nd_xCoIn_5$, the typical signature of quantum criticality (i.e., divergence of C/T at low T) is likely hidden by SC and by the upturn in C/T. We also note that the highest T_c achieved in $Ce_{0.95}Nd_{0.05}RhIn_5$, $T_c^{max} = 1.85$ K, is 0.4 K lower than T_c^{max}

of CeRhIn$_5$. This same suppression of T_c^{max} is observed in $Ce_{0.95}Nd_{0.05}CoIn_5$ and indicates that Nd ions act similarly as magnetic pair-breaking impurities.

To further investigate the nature of the Nd-induced magnetism, we turn to the field-dependent heat capacity data. Fig. 3A shows C_{ac}/T vs. T at 1.85 GPa ($>P_{c1}$) and low magnetic fields. The zero-field transition at $T_N^{Nd} = 0.96$ K remains unchanged in a field of 2.5 kOe. As the field is increased further, however, the specific heat anomaly splits, one anomaly moving to lower temperatures and the other moving to higher temperatures. At 11 kOe, our data show features at 1 K and 0.7 K. Previous reports on CeRhIn$_5$ at similar pressures ($\sim$1.9 GPa) show that the field-induced transition emerges at $T_N = 1$ K when $H = 11$ kOe (33). It is thus reasonable to associate the anomaly we observe at 1 K and 11 kOe with the field-induced magnetism in CeRhIn$_5$. Further, Fig. 3B shows the high-H evolution of T_N with a field dependence very similar to that of CeRhIn$_5$: T_N first increases with H and then remains constant above the upper critical field H_{c2}. As shown in the H–T phase diagram (Fig. 3C), this field-induced T_N clearly competes with T_N^{Nd}, as reflected in the rapid suppression of T_N^{Nd} as a function of H. In fact, no evidence for T_N^{Nd} is observed at fields $H \geq 22$ kOe, implying a field-induced quantum-critical point in addition to the pressure-induced, zero-field critical point of this order. Due to the reasons explained above, our results strongly point to two distinct types of magnetism emerging in $Ce_{0.95}Nd_{0.05}RhIn_5$. The first one is due to Nd ions, and it has the hallmarks of that in $Ce_{0.95}Nd_{0.05}CoIn_5$. The second is the H-induced magnetism that appears in pure CeRhIn$_5$ (23, 27).

Discussion

What is the role of Nd and why is it special? At a concentration of 5%, average spacing of 17 Å and nonperiodic distribution on Ce sites, Nd is too dilute to induce magnetic order by dipole or indirect Ruderman–Kittel–Kasuya–Yosida interactions. Its role, then, must be more subtle. Using the bulk modulus of CeRhIn$_5$ and the unit cell volume variation in $Ce_{1-x}Nd_xRhIn_5$, we estimate that $Ce_{0.95}Nd_{0.05}RhIn_5$ experiences an effective chemical pressure of $\Delta P = 0.25$ GPa relative to CeRhIn$_5$ (29). From the phase diagram of CeRhIn$_5$, this ΔP would increase T_N by 0.1 K instead of producing the observed reduction. Hence, we conclude that chemical pressure per se is not the dominant tuning parameter.
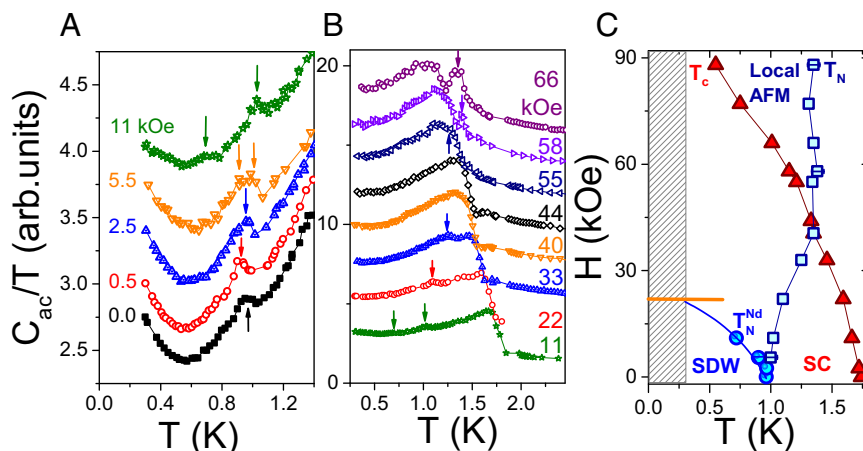
Fig. 3. AC heat capacity, C_{ac}, of $Ce_{0.95}Nd_{0.05}RhIn_5$ (s2) at 1.85 GPa. (*A*) T dependence of C_{ac}/T at low fields. An offset of 0.2 has been added for clarity. (*B*) T dependence of C_{ac}/T at high fields. (*C*) H–T phase diagram. The diagonal bars delimit the inaccessible temperature region in our experiments ($T < 0.3$ K). The solid horizontal line at $H = 22$ kOe indicates that no transition T_N^{Nd} is observed above 0.3 K for this field. We note that only T_N^{Nd} is observed at zero field. The field-induced T_N emerges at 11 kOe, as in pure CeRhIn$_5$.
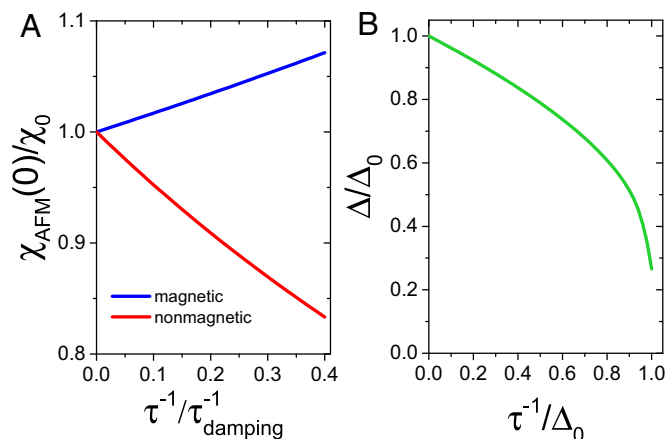
Fig. 4. (*A*) Static spin susceptibility $\chi_{AFM}(\mathbf{Q}, \omega = 0)$ as function of the total impurity scattering rate for the cases of nonmagnetic (red curve) and paramagnetic impurities (blue curve). (*B*) The suppression of the effective SC gap Δ by both magnetic and nonmagnetic impurities. In these plots, we considered point-like impurities. Here, Δ_0 is the gap of the clean system whereas $\tau_{damping}^{-1}$ is the Landau damping (see *Supporting Information* for details).

The disruption of lattice periodicity by substituting Ce ions with magnetic Nd ions contributes to reducing T_N at zero pressure (29). This conclusion is supported by the observation that nonmagnetic La substitution for Ce in CeRhIn$_5$ also depresses T_N similarly (31, 34). The weak depression of T_N and concomitant incremental increase in residual resistivity with Nd substitution by themselves cannot account for the observed zero-field magnetic order above P_{c1}^*. Neodymium, however, carries an additional magnetic moment that is unlikely to be quenched by Kondo screening. In the context of CeCoIn$_5$, Michal and Mineev (18) proposed that the Q phase observed in the presence of an in-plane magnetic field is the consequence of the condensation of the spin-exciton collective mode found in the SC phase. Thus, it is natural to consider whether the Nd magnetic moments immersed in CeRhIn$_5$ at zero field could also promote a similar behavior.

As discussed in detail in *Supporting Information* (Figs. S2 and S3), condensation of spin excitons takes place when the spin-resonance-mode frequency ω_{res} vanishes. Within a random-phase approximation (RPA) approach, ω_{res} is given by the pole of the renormalized magnetic susceptibility, i.e., when $\chi_{AFM}(\mathbf{Q}, \omega_{res}) = 1/U$, where U is the effective electronic interaction projected in the SDW channel and $\chi_{AFM}(\mathbf{Q}, \omega_{res})$ is the noninteracting magnetic susceptibility inside the SC state. When the ordering vector $\mathbf{Q}$ connects points of the Fermi surface with different signs of the SC gap, $\Delta_{\mathbf{k}} = -\Delta_{\mathbf{k+Q}}$, $\chi_{AFM}(\mathbf{Q}, \omega)$ generically diverges when $\omega \to 2\Delta$ and remains nonzero when $\omega \to 0$. Thus, even a very weak U can, in principle, induce a resonance mode with frequency near 2Δ. Once the interaction increases, ω_{res} moves to lower frequencies. When the interaction overcomes a critical value, $U > U_c \equiv \chi_{AFM}^{-1}(\mathbf{Q}, 0)$, the resonance mode vanishes and SDW order is established inside the SC dome.

In our case, the interaction U is presumably independent of pressure. Thus, in order for magnetic impurities to promote spin-exciton condensation, $\chi_{AFM}(\mathbf{Q}, 0)$ must increase (i.e., the critical interaction value U_c must decrease) as a function of the impurity potential. To investigate whether this is a sensible scenario, we considered a toy model consisting of two "hot spots" located at momenta $\mathbf{k}$ and $\mathbf{k} + \mathbf{Q}$ at the Fermi surface such that $\Delta_{\mathbf{k}} = -\Delta_{\mathbf{k+Q}}$. Note that such a hot spots model has been previously used to study the effects of disorder on SC (35). To focus on the general properties of the model, we linearize the band

dispersion around the hot spots and compute both $\chi_{AFM}(\mathbf{Q}, 0)$ and the effective gap amplitude Δ at $T = 0$ as function of the total impurity scattering rate τ^{-1} within the self-consistent Born approximation (similarly to what was done in ref. 36 for s^{+-} SC and perfectly nested bands). As shown in Fig. 4, whereas both magnetic and nonmagnetic impurity scattering suppress Δ at the same rate (Fig. 4*B*), we find that $\chi_{AFM}(\mathbf{Q}, 0)$ is suppressed for nonmagnetic impurity but enhanced by magnetic impurity scattering (Fig. 4*A*). Thus, in the case of nonmagnetic impurities, although the resonance-mode frequency may decrease compared with the clean case, it never collapses to zero. Because magnetic impurity scattering enhances $\chi_{AFM}(\mathbf{Q}, 0)$ but does not necessarily destroy SC, the system may undergo an SDW transition inside the SC dome. Although the fate of the system will depend on microscopic details beyond those captured by the toy model considered here, our model nicely illustrates that it is plausible for magnetic impurity scattering to drive spin-exciton condensation in the SC phase. In this regard, we note that previous investigations of a microscopically motivated theoretical model also found that the Q phase may be stabilized by magnetic impurities even at zero external field (37).

These results suggest that other magnetic impurities could induce the same type of SDW order in both CeCoIn$_5$ and pressurized CeRhIn$_5$. In fact, we show, in *Supporting Information* (Fig. S1), that easy-plane Gd^{3+} ions ($J = S = 7/2$) also induce a transition in the heat capacity data of both Co and Rh members. This anomaly is similar to the one induced by easy-axis (c-axis) Nd^{3+} ions ($J = 9/2$, $L = 3$, $S = 3/2$) discussed above. Hence, Nd is not "special" in inducing magnetic order in the superconducting states of Ce$_{0.95}$Nd$_{0.05}$CoIn$_5$ and Ce$_{0.95}$Nd$_{0.05}$RhIn$_5$, and other unconventional superconductors that host a spin resonance mode may also display zero-field magnetism via the same mechanism. Our results also imply that nonmagnetic impurities will not induce condensation of excitations, in agreement with experimental data on La-substituted CeRhIn$_5$ (34, 38, 39).

Finally, we note that the SDW ordering vector in Nd-doped CeCoIn$_5$ corresponds closely to the nodal structure (12) that is also found in the superconducting state of CeRhIn$_5$ (10). Hence, the magnetic wavevector of zero-field order above P_{c1}^* in Ce$_{0.95}$Nd$_{0.05}$RhIn$_5$ should also be close to $\mathbf{Q} = (0.45, 0.45, 0.5)$. As argued in ref. 12, field-induced magnetism in CeCoIn$_5$ (Q phase) also appears to be a consequence of the condensation of the spin resonance mode. We, therefore, expect neutron scattering experiments to find a spin resonance of c-axis character below T_c in CeRhIn$_5$ at $P > P_{c1}$.

Conclusion

In summary, we generalize the observation of Nd-induced magnetism in CeCoIn$_5$ to pressurized CeRhIn$_5$ and Gd-substituted members. This SDW order, which reflects the nodal gap symmetry, is argued to be a consequence of the condensation of spin excitations that arise inside the SC state. Given the several similarities between CeCoIn$_5$ and Ce$_2$PdIn$_8$ (40), Nd substitution might nucleate AFM order in its superconducting state. Appropriate substitutions in other unconventional superconductors that host a spin resonance also should induce zero-field magnetism by the same mechanism, and magnetism should be tunable to a quantum-critical point inside their SC phase.

Materials and Methods

The series Ce$_{1-x}$Nd$_x$RhIn$_5$ was grown by the In-flux technique, and its properties are reported elsewhere (29). Crystals with $x = 0.05$ and free of unreacted In were mounted in a hybrid piston–cylinder pressure cell, filled with silicone fluid as the pressure medium, and a piece of Pb whose change in T_c served as a manometer. Gs-substituted crystals were grown using the same method. Electrical resistivity was measured by a four-probe method with current flow in the *ab* plane. Semiquantitative heat capacity was obtained by an AC

calorimetry technique described elsewhere (41). Magnetic fields to 9 T were applied parallel to the *ab* plane. The results above have been reproduced in different crystals, and, for clarity, we show resistivity and calorimetry data for two representative samples labeled sample 1 (s1) and sample 2 (s2).

1. Monthoux P, Pines D, Lonzarich GG (2007) Superconductivity without phonons. *Nature* 450:1177–1183.
2. Scalapino DJ (2012) A common thread: The pairing interaction for unconventional superconductors. *Rev Mod Phys* 84:1383–1417.
3. Schilling A, Cantoni M, Guo JD, Ott HR (1993) Superconductivity above 130 K in the Hg-Ba-Ca-Cu-O system. *Nature* 363:56–58.
4. Stewart GR. Superconductivity in iron compounds (2011) *Rev Mod Phys* 83:1589–1652.
5. White BD, Thompson JD, Maple MB (2015) Unconventional superconductivity in heavy-fermion compounds. *Physica C* 514:246–278.
6. Eschrig M (2006) The effect of collective spin-1 excitations on electronic spectra in high-T_c superconductors. *Adv Phys* 55:47–53.
7. Yu G, Li Y, Motoyama EM, Greven M (2009) A universal relationship between magnetic resonance and superconducting gap in unconventional superconductors. *Nat Phys* 5:873–875.
8. Park WK, Sarrao JL, Thompson JD, Greene LH (2008) Andreev reflection in heavy-fermion superconductors and order parameter symmetry in $CeCoIn_5$. *Phys Rev Lett* 100:177001.
9. Zhou BB, et al. (2013) Visualizing nodal heavy fermion superconductivity in $CeCoIn_5$. *Nat Phys* 9:474–479.
10. Park T, Bauer ED, Thompson JD (2008) Probing the nodal gap in the pressure-induced heavy fermion superconductor $CeRhIn_5$. *Phys Rev Lett* 101:177002.
11. Stock C, Broholm C, Hudis J, Kang HJ, Petrovic C (2008) Spin resonance in the *d*-wave superconductor $CeCoIn_5$. *Phys Rev Lett* 100:087001.
12. Raymond S & Lapertot G (2015) Ising incommensurate spin resonance of $CeCoIn_5$: A dynamical precursor of the *Q* phase. *Phys Rev Lett* 115:037001.
13. Panarin J, Raymond S, Lapertot G, Flouquet J (2009) Evolution of the spin resonance in $CeCoIn_5$ under magnetic field. *J Phys Soc Jpn* 78:113706.
14. Stock C, et al. (2012) Magnetic field splitting of the spin resonance in $CeCoIn_5$. *Phys Rev Lett* 109:167207.
15. Young BL, et al. (2007) Microscopic evidence for field-induced magnetism in $CeCoIn_5$. *Phys Rev Lett* 98:036402.
16. Kenzelmann M, et al. (2008) Coupled superconducting and magnetic order in $CeCoIn_5$. *Science* 321:1652–1654.
17. Kenzelmann M, et al. (2010) Evidence for a magnetically driven superconducting *Q* phase of $CeCoIn_5$. *Phys Rev Lett* 104:127001.
18. Michal VP, Mineev VP (2011) Field-induced spin-exciton condensation in the $d_{x^2-y^2}$-wave superconductor $CeCoIn_5$. *Phys Rev B* 84:052508.
19. Hu R, Lee Y, Hudis J, Mitrovic VF, Petrovic C (2008) Composition and field-tuned magnetism and superconductivity in $Nd_{1-x}Ce_xCoIn_5$. *Phys Rev B* 77:165129.
20. Raymond S, et al. (2014) Magnetic order in $Ce_{0.95}Nd_{0.05}CoIn_5$: The *Q*-phase at zero magnetic field. *J Phys Soc Jpn* 83:013707.
21. Lake B, et al. (2002) Antiferromagnetic order induced by an applied magnetic field in a high-temperature superconductor. *Nature* 415:299–302.
22. Demler E, Sachdev S, Zhang Y (2001) Spin-ordering quantum transitions of superconductors in a magnetic field. *Phys Rev Lett* 87:067202.
23. Park T, et al. (2006) Hidden magnetism and quantum criticality in the heavy fermion superconductor $CeRhIn_5$. *Nature* 440:65–68.
24. Bao W, et al. (2000) Incommensurate magnetic structure of $CeRhIn_5$. *Phys Rev B* 62:R14621–R14624.
25. Hegger H, et al. (2000) Pressure-induced superconductivity in quasi-2D $CeRhIn_5$. *Phys Rev Lett* 84:4986–4989.
26. Mito T, et al. (2003) Coexistence of antiferromagnetism and superconductivity near the quantum criticality of the heavy-fermion compound $CeRhIn_5$. *Phys Rev Lett* 90:077004.
27. Knebel G, Aoki D, Braithwaite D, Salce B, Flouquet J (2006) Coexistence of antiferromagnetism and superconductivity in $CeRhIn_5$ under high pressure and magnetic field. *Phys Rev B* 74:020501.
28. Pham LD, Park T, Maquilon S, Thompson JD, Fisk Z (2006) Reversible tuning of the heavy-fermion ground state in $CeCoIn_5$. *Phys Rev Lett* 97:056404.
29. Rosa PFS, Oostra A, Thompson JD, Pagliuso PG, Fisk Z (2016) Unusual Kondo-hole effect and crystal-field frustration in Nd-doped $CeRhIn_5$. *Phys Rev B* 94:045101.
30. Anderson AC, Holmstrom B, Krusius M, Pickett GR (1969) Calorimetric investigation of the hyperfine interactions in metallic Nd, Sm, and Dy. *Phys Rev* 183:546–552.
31. Pagliuso PG, et al. (2002) Ce-site dilution studies in the antiferromagnetic heavy fermions $Ce_mRh_nIn_{3m+2n}$ (*m* = 1, 2; *n* = 0, 1). *Phys Rev B* 66:054433.
32. Bauer ED, et al. (2011) Electronic inhomogeneity in a Kondo lattice. *Proc Natl Acad Sci USA* 108:6857–6861.
33. Park T, Thompson JD (2009) Magnetism and superconductivity in strongly correlated $CeRhIn_5$. *New J Phys* 11:055062.
34. Mendonça-Fereira L, et al. (2008) Tuning the pressure-induced superconducting phase in doped $CeRhIn_5$. *Phys Rev Lett* 101:017005.
35. Kang J, Fernandes RM (2016) Robustness of quantum critical pairing against disorder. *Phys Rev B* 93:224514.
36. Maiti S, Knolle J, Eremin I, Chubukov AV (2011) Effect of nodes, ellipticity, and impurities on the spin resonance in iron-based superconductors. *Phys Rev B* 84:144524.
37. Martiny JHJ, Gastiasoro MN, Vekhter I, Andersen BM (2015) Impurity-induced antiferromagnetic order in Pauli-limited nodal superconductors: Application to heavy-fermion $CeCoIn_5$. *Phys Rev B* 92:224510.
38. Panarin J, Raymond S, Lapertot G, Flouquet J, Mignot JM (2011) Effects of nonmagnetic La impurities on the spin resonance of $Ce_{1-x}La_xCoIn_5$ single crystals as seen via inelastic neutron scattering. *Phys Rev B* 84:052505.
39. Nakatsuji S, et al. (2002) Intersite coupling effects in a Kondo lattice. *Phys Rev Lett* 89:106402.
40. Dong JK, et al. (2011) Field-induced quantum critical point and nodal superconductivity in the heavy-fermion superconductor Ce_2PdIn_8. *Phys Rev X* 1:011010.
41. Sidorov VA, Thompson JD, Fisk Z (2010) Magnetic transitions in a heavy-fermion antiferromagnet U_2Zn_{17} at high pressure. *J Phys Condens Matter* 22:406002.